Uranyl-citrate Speciation Diagram in Aqueous Solutions.

Theoretical and Capillary Electrophoresis Studies at 25 ℃

Sondes Boughammoura, Jalel M'halla*

Laboratoire d'Electrochimie des solutions, Faculté des sciences, Universit éde Monastir

5000 Monastir, Tunisia

*jalel.mhalla@fsm.rnu.tn

***Abstract*-In this study, we develop new analytical and numerical speciation calculations corresponding to all kinds of combinations of complexation constants and hydrolysis constants given by more or less reliable literature data, and associated to fifteen probable uranyl-citrate species: M_pL_n, (with: $M \equiv (UO_2)^{2+}$, $L \equiv (HCit)^{3-}$ and p = 1, 2; n = 1, 2, 3), $M_pL_nH_m$, (p = 1, 2; n = 1, 2; m = 1, 2, 4), $M_p(OH)_q$, (p = 1- 4; q = 1-7), $M_pL_nH_m(OH)_q$, (p = 1, 2; n = 1, 2; m = 1, 2; q = 1, 2) as well as to the "improbable": $[(UO_2)H_2(HCit)_2]^{2-}$ specie (reported by only one reference), in order to analyse deeply their impact on the speciation diagram of U(VI) in citrate aqueous solutions at 25 ℃, in a wide range of pH and for citrate to uranium ratios R_c = U(VI)/Citrate equal to 0.02, 1 and 2. The main result of this work is that, although the employed combinations present some significant dispersions, they leads to the same result: the hydrolyzed monomer $[(UO_2)H(HCit)(OH)]^-$, the hydrolyzed dimer $[(UO_2)_2H_2(HCit)_2(OH)_2]^{2-}$ and the monomer $(UO_2)(HCit)]^-$ are largely predominant in the pH range of our interest (2< pH< 5.5), by comparison to the percentages of the other species presumably existing (except the $[(UO_2)H_2(HCit)_2]^{2-}$ specie). This investigation is therefore a supplementary proof of the reliability of the processes of protonation and hydrolysis of both the monomer and the dimer: $[(UO_2)(HCit)]^-$, $[(UO_2)_2(HCit)_2]^{2-}$ detected via the experimental electropherograms obtained by the capillary electrophoresis method which was used because of its capacity to separate the different hydrolysis products of the anionic U(VI)-citrate complexes. Consequently, it is thus possible to underline that the hydrolysis of UO_2^{2+} which generally occurs at relatively elevated pH is facilitated at lower pH by the citrate complexation followed by the protonation.**

Keywords-Uranium; Citrate; Speciation ; Electrophoresis; Analytical ; Numerical

I INTRODUCTION

The ability of uranium to form strong stable complexes with organic compounds has been extensively utilized for cleaning up uranium contamination in soils and in the nuclear industry. Citric acid is a common constituent which forms strong water soluble complexes with U(VI) and U(IV) over a wide range of pH. The U(VI) citrate complexes have already been investigated in several experimental and modelling studies [1,2,5,6,10]. Accordingly, it was concluded that citrate has a strong affinity for uranium. However, it was also shown that this affinity varies with the experimental method, the ionic strength, the pH and the stoichiometry of the ($M \equiv U(VI) \equiv UO_2^{2+}$)/($L \equiv$ ligand $\equiv HCit^{3-}$) ratio. This dependence could partially explain the fact that the reported data by the literature concerning the different stability constants β_{pn} for M_pL_n complexes scatter markedly. In fact, the M_pL_n complexes could exist under different protonation and hydrolysis states: $M_pL_nH_m$ and $M_pL_nH_m(OH)_q$. However, most of the analytical techniques cannot differentiate between these different states. From recent analysis of all the previous works [8-10], a limited number of U (VI) citrate complexes have been selected ($[(UO_2)(HCit)]^-$, $[(UO_2)_2(HCit)_2]^{2-}$, $[(UO_2)H(HCit)]$) and their corresponding stability constants β_{pnm} re-determined. More recently [16], we have underlined the advantage of the capillary electrophoresis technique over most of the speciation methods previously used because it should give the possibility to specify all the anionic $M_pL_nH_m(OH)_q$ entities, by separating them on the basis of the differences in their electrophoretic mobility even at low concentration closer to the level found in nature. Accordingly, we have assigned some three peaks found in the absorbance spectra of our capillary electrophoresis experiments for pH < 5, to the following three species: the U(VI)-citrate monomer, the hydrolysis product of this monomer complex: $[(UO_2)H(HCit)(OH)]^-$ and the dimer of the hydrolysis product: $[(UO_2)_2H_2(HCit)_2(OH)_2]^{2-}$. The latter two species were postulated in reference [2] and therefore play a crucial role in our speciation calculations despite the controversy concerning them from a chemical point of view. In particular, we have signalled for pH >3 the occurrence of an inverted tendency accompanied by a strong modification of the calculated speciation diagrams when we take into account these hydrolysed complexes via their corresponding constants: β_{1111} and β_{2222}. Indeed, the use of these additional constants leads to a completely different U(VI) distribution so that 60-70% of uranium is present in the form of hydrolyzed monomer rather than $[(UO_2)_2(HCit)_2]^{2-}$ and 20-30% in the form of hydrolyzed dimmer rather than $[(UO_2)(HCit)]^-$. Notice that the speciation diagrams given in our previous work paper (in the absence and in the presence of the hydrolyzed monomer and dimmer) are calculated on the basis of two constants: β_{11} and β_{22} selected among some published sets of values currently "more or less" established. However, in spite of the detection of the three peaks above mentioned, this inverted tendency is not quantitatively completely in agreement with the electropherograms results and we have explained this difference in assuming that the protonation and hydrolysis effects are non-reproducible kinetic processes.

Instead, we will expose in the present work, new speciation calculations corresponding to all kinds of combinations of complexation constants given by more or less reliable literature data, and associated to fifteen probable species: M_pL_n, $M_pL_nH_m$, $M_p(OH)_q$, $M_pL_nH_m(OH)_q$, as well as to the "improbable": $[(UO_2)H_2(HCit)_2]^{2-}$ specie (reported by only one reference), in order to analyse deeply their impact on the speciation diagram of U(VI) in citrate aqueous solutions. In the first step of this study we will therefore investigate theoretically (analytically and numerically) the different

speciation diagrams obtained at 25 ℃, in a wide range of pH and for different citrate to uranium ratios, following the use partly or completely of the uranyl-citrate complexes and uranyl- hydroxides mentioned above, and in assuming that the different reactions of complexation, protonation and hydrolysis have reached their complete chemical equilibrium. In the second step, we will compare the similarities and the differences between them in the perspective of verifying the fact that: for the pH range of our interest (2< pH< 5.5), despite their dispersion, the use of the several sets of values (more or less reliable), of the different complexation constants given by the literature, confirms the large predominance of the hydrolyzed monomer: $[(UO_2)H(HCit)(OH)]^-$ and of the hydrolyzed dimer: $[(UO_2)_2H_2(HCit)_2(OH)_2]^{2-}$ by comparison to the percentages of the other species presumably existing (except the $[(UO_2)H_2(HCit)_2]^{2-}$ specie). This investigation could be therefore considered as a supplementary proof of our previous interpretation of the experimental electropherograms obtained by the capillary electrophoresis method (in particular the reliability of the processes of protonation and hydrolysis of both the monomer and the dimer: $[(UO_2)(HCit)]^-$, $[(UO_2)_2(HCit)_2]^{2-}$), and also as a test of the validity of the different literature data as well as of the assumption of the chemical equilibrium.

II METHOD OF CALCULATION

A. Definitions

We will designate in the following definitions by $[X_i]$ the molar concentration of specie i and by γ_{Xi} the activity coefficient of X_i in the Henry reference in water at 25 ℃ which is related to the ionic strength I according to the generalized Debye equation [γ] :

$$\log(\gamma_{Xi}) = -0.5115(Z_i)^2 I^{1/2}/(1 + 1.5I^{1/2}) + \Sigma_j e_{ij}(C_j) \quad (1)$$

$$I = 0.5\Sigma_j(Z_j)^2 C_j \quad (2)$$

where Z_j and C_j are respectively the valence and the molar concentration of the j species, and e_{ij} is a specific interaction coefficient between species i and j.

1) Complexation

We define the complexation constant β'_{pn} and the apparent complexation constant β_{pn} corresponding to the following complexation equilibrium respectively by:

$$pM + nL \Leftrightarrow M_pL_n \quad : \quad \beta_{pn} = [M_pL_n][L]^{-n}[M]^{-p} \quad (3a)$$

$$\beta'_{pn} = (\gamma_{MpLn})(\gamma_L)^{-n}(\gamma_M)^{-p}\beta_{pn} \quad (3b)$$

2) Protonation

We define the protonation constant β'_{pnm} and the apparent protonation constant β_{pnm} corresponding to the following protonation equilibrium respectively by:

$$M_pL_n + mH^+ \Leftrightarrow M_pL_nH_m \quad : \quad \beta_{pnm} = [M_pL_nH_m][M_pL_n]^{-1}[H^+]^{-m} \quad (4a)$$

$$\beta'_{pnm} = (\gamma_{MpLnHm})(\gamma_{MpLn})^{-1}(\gamma_{H^+})^{-m}\beta_{pnm} \quad (4b)$$

3) Hydrolysis

We define the hydrolysis constant β'_{pnmq} and the apparent hydrolysis constant β_{pnmq} corresponding to the following hydrolysis equilibrium respectively by:

$$M_pL_nH_m + qH_2O \Leftrightarrow M_pL_nH_m(OH)_q + qH^+ \quad : \quad \beta_{pnmq} = [M_pL_nH_m(OH)_q][H^+]^q[M_pL_nH_m]^{-1} \quad (5a)$$

$$\beta'_{pnmq} = (\gamma_{MpLnHm(OH)q})(\gamma_{H^+})^q(\gamma_{MpLnHm})^{-1}\beta'_{pnmq} \quad (5b)$$

a) Peculiar Case (n = 0; m = 0)

We define the hydrolysis constant $KH'_{pq'}$ of the metallic ion M and the apparent hydrolysis constant $KH_{pq'}$ corresponding to the following hydrolysis equilibrium respectively by:

$$pM + q'OH^- \Leftrightarrow M_p(OH)_{q'} \quad : \quad KH_{pq'} = [M_p(OH)_{q'}][OH^-]^{q'}[M]^{-p} \quad (6a)$$

$$KH'_{pq'} = (\gamma_{Mp(OH)q'})(\gamma_{OH^-})^{-q'}(\gamma_M)^{-p}KH_{pq'} \quad (6b)$$

4) Acidity

We define the acidity constant $K^{a'}{}_l$ and the apparent acidity constant $K^a{}_l$ corresponding to the following equilibrium respectively by:

$$L + lH^+ \Leftrightarrow H_lL \quad : \quad K^a{}_l = [H_lL][L]^{-1}[H^+]^{-l} \quad (7a)$$

$$K^{a'}{}_l = (\gamma_{HlL})(\gamma_L)^{-1}(\gamma_{H^+})^{-l}K^{a'}{}_l \quad (7b)$$

III EXPRESSIONS OF THE SPECIES CONCENTRATIONS IN TERMS OF [M], [L] AND [H+]

A. General Expressions

The expressions of the different species concentrations in terms of [M] and [L] concentrations are given by:

$$[M_pL_n] = \beta_{pn}[M]^p[L]^n \quad (8)$$

$$[M_pL_nH_m] = \beta_{pnm}\beta_{pn}[M]^p[L]^n[H^+]^m \quad (9)$$

$$[M_pL_nH_m(OH)_q] = \beta_{pnmq}\beta_{pnm}\beta_{pn}[M]^p[L]^n[H^+]^m[H^+]^{-q} \quad (10)$$

$$[M_p(OH)_{q'}] = (KH_{pq'})[OH^-]^{q'}[M]^p \quad (11)$$

$$[H_lL] = (K^a{}_l)[L][H^+]^l \quad (12)$$

B. Equations of Conservation

If we define $C°_M$ and $C°_L$ as, respectively, the total concentrations of M and L, thus:

$$C°_M = [M] + \sum_p p[M]^p\{\sum_n(\beta_{pn} + \sum_m\beta_{pnm}\beta_{pn}[H^+]^m + \sum_m\sum_q \beta_{pnmq}\beta_{pnm}\beta_{pn}[H^+]^m[H^+]^{-q})[L]^n\} + \sum_p p[M]^p\{\sum_{q'}(KH_{pq'})(K_W)^{q'}[H^+]^{-q'}\} \quad (13)$$

$$C°_L = \sum_p[M]^p\{\sum_n n(\beta_{pn} + \sum_m\beta_{pnm}\beta_{pn}[H^+]^m + \sum_m\sum_q\beta_{pnmq}\beta_{pnm}\beta_{pn}[H^+]^m[H^+]^{-q})[L]^n\} + \{1+\sum_l(K^a{}_l)H^+]^l\}[L] \quad (14)$$

KW = [H+][OH-] is the apparent ionization constant of water.

Now, if we note: $x \equiv [M]$ and $y \equiv [L]$, we will obtain the following equations:

$$C°_M = x + \sum_p px^p\sum_n A_{np}y^n + \sum_p px^p E + \{1+\sum_l(K^a{}_l)H^+]^l\}[L] \quad (15)$$

$$C°_L = \sum_p x^p\sum_n nA_{np}y^n + Dy \quad (16)$$

With : $A_{np} = (\beta_{pn} + \sum_m\beta_{pnm}\beta_{pn}[H^+]^m + \sum_m\sum_q\beta_{pnmq}\beta_{pnm}\beta_{pn}[H^+]^m[H^+]^{-q})$ (17)

$$E_p = [\sum_{q'}(KH_{pq'})(K_W)^{q'}[H^+]^{-q'}] \quad (18)$$

$$D = \{1+\sum_l(K^a{}_l)[H^+]^l\} \quad (19)$$

Note that the parameters A_{np}, E_p and D depend on the different apparent equilibrium constants and are function on the ionic strength $I = 0.5\Sigma_i(Z_i)^2C_i$ and pH. We proceed therefore to a recurrent self consistent method: As a first approximation we equal the apparent constants to their corresponding thermodynamic constants, we calculate therefore for a given pH, the parameters A_{np}, E_p and D according Eqs. (17-19) in order to obtain a system of two equations with two variables: x and y according Eqs.(15-16). The resolution of this system for a given total concentrations $C°_M$ and $C°_L$ allows us to calculate the different concentrations of all the species present in solution: $[M_pL_n]$, $[M_pL_nH_m]$, $[M_pL_nH_m(OH)_q]$,$[M_p(OH)_{q'}]$ and $[H_lL]$ according Eqs.(8-12) and therefore all the activity coefficients via the ionic strength I. In the second step we recalculate the new apparent constants via Eqs. (3b -7b) and we repeat the procedure until convergence.

The resolution of the algebraic system at each step is achieved using a basic numerical program involving n successive buckles and verifying the convergence conditions:$[(x_n - x_{n-1}) /x_n] \leq 10^{-5}$ and $[(y_n - y_{n-1})/x_n] \leq 10^{-5}$. This method allows us to establish for a given $C°_M$ and $C°_L$, the corresponding speciation diagram giving the variation of the fraction in % of the different species with the pH.

IV THEORETICAL URANYL-CITRATE SPECIATION DIAGRAM IN AQUEOUS SOLUTIONS

Now, we will apply this general method in the case of:

$M \equiv (UO_2)^{2+}$, $L \equiv (HCit)^{3-}$, in order to obtain the speciation diagram of Uranyl-Citrate complexes in aqueous solutions. For this, we will use different literature data for the calculation of β_{pnmq}, β_{pnm}, β_{pn}, $(K_pH_{q'})$ and $(K^a{}_l)$ constants.

A. The Most Probable Uranyl-Citrate Complexes in Aqueous Solutions

The most probable uranyl species present in citrate aqueous solutions, according to the literature [2,3,7,10], are collected in Table 1.

B. Calculation of βpnmq, βpnm and βpn Constants from Literature Data

In order to calculate β_{pnmq} and β_{pnm} constants, we proceeded as follows:

According to the recent and less recent literature data [2,3,7,10], we can calculate the four protonation constants (β_{111}), (β_{112}) (β_{122}) , (β_{224}) and the two generalized constants (β_{1111}) and (β_{2222}), in terms of the intermediate constants (K_I), (K_{2I}), (K_{22I}), (K_{224I}), (K_{II}) and (K_{III}) corresponding to the equilibria given in Table 2.

TABLE 1 THE DIFFERENT URANYL SPECIES FORMED IN CITRATE AQUEOUS SOLUTIONS

Complexes: β_{pn}	Protonated complexes: β_{pnm}	Uranyl hydroxides: $KH_{pq'}$	General hydrolyzed complexes: β_{pnmq}
$[(UO_2)(HCit)]^-$	$[(UO_2)H(HCit)]$	$[(UO_2)(OH)]^+$	$[(UO_2)H(HCit)(OH)]^-$
$[(UO_2)(HCit)_2]^{4-}$	$[(UO_2)H_2(HCit)]^+$	$[(UO_2)(OH)_2]$	$[(UO_2)_2H_2(HCit)_2(OH)_2]^{2-}$
$[(UO_2)_2(HCit)_2]^{2-}$	$[(UO_2)H_2(HCit)_2]^{2-}$	$[(UO_2)(OH)_3]^-$	
$[(UO_2)_2(HCit)_3]^{5-}$	$[(UO_2)_2H_2(HCit)_2]$	$[(UO_2)_2(OH)]^{3+}$	
	$[(UO_2)_2H_4(HCit)_2]^{2+}$	$[(UO_2)_2(OH)_2]^{2+}$	
		$[(UO_2)_3(OH)_4]^{2+}$	
		$[(UO_2)_3(OH)_5]^+$	
		$[(UO_2)_3(OH)_7]^-$	
		$[(UO_2)_4(OH)_7]^+$	

TABLE 2 HYDROLYSIS AND COMPLEXATION CONSTANTS OF URANIUM AT 25 °

Equilibrium	log(K) : Ref [2]	log(K) : Ref [10]
$(UO_2)^{2+} + H(HCit)^{2-} \Leftrightarrow [(UO_2)H(HCit)]$	$\log(K_I) = 6.0$ (I = 0.136)	$\log(K_I) = 4.23$ (I = 0.1)
$(UO_2)^{2+} + H_2(HCit)^- \Leftrightarrow [(UO_2)H_2(HCit)]^+$		$\log(K_{2I}) = 2.79$ (I = 0.1)
$(UO_2)^{2+} + 2[H(HCit)]^{2-} \Leftrightarrow [(UO_2)H_2(HCit)_2]^{2-}$		$\log(K_{22\,I}) = 11.2$ (I = ?)
$2(UO_2)^{2+} + 2[H_2(HCit)]^- \Leftrightarrow [(UO_2)_2H_4(HCit)_2]^{2+}$		$\log(K_{224\,I}) = 8.9$ (I = 1)
$(UO_2)^{2+} + [H(HCit)]^{2-} + H_2O \Leftrightarrow [(UO_2)H(HCit)(OH)]^- + H^+$	$\log(K_{II}) = 2.84$ (I = 0.136)	
$2(UO_2)^{2+} + 2[H(HCit)]^{2-} + 2H_2O \Leftrightarrow [(UO_2)_2H_2(HCit)_2(OH)_2]^{2-} + 2H^+$	$\log(K_{III}) = 7.68$ (I = 0.136) and 9.04 (I = 0.)	

The different expressions of the β_{pnm} and β_{pnmq} constants are summarized in "Table 3".

TABLE 3 EXPRESSIONS OF BPNMQ AND BPNM CONSTANTS OF URANYL-CITRATE COMPLEXES

β_{111}	β_{1111}	β_{112}
$(K^a{}_1)(K_I)(\beta_{11})^{-1}$	$(K_{II})(K_I)^{-1}$	$(K^a{}_2)(K_{21})(\beta_{11})^{-1}$
β_{122}	$\beta_{222}\beta_{2222}$	β_{224}
$(K^a{}_1)^2(K_{22\,I})(\beta_{12})^{-1}$	$(K_{III})(K^a{}_1)^2(\beta_{22})^{-1}$	$(K^a{}_2)^2(K_{224\,I})(\beta_{22})^{-1}$

C. Equations of Conservation in the Case of the Uranium Complexation with Citric Acid

According to the data given in Table 1, the most probable values for p, n, m and q are: p = 1, 2; n = 1,2 ; m = 1,4; and q = 1,2 ; the corresponding parameters A_{np} and E_p are thus:

$$A_{11} \equiv A = (\beta_{11} + \beta_{111}\,\beta_{11}\,[H^+] + \beta_{112}\,\beta_{11}\,[H^+]^2 + \beta_{1111}\,\beta_{111}\,\beta_{11}) \quad (20)$$

$$A_{21} = (\beta_{12} + \beta_{122}\,\beta_{12}\,[H^+]^2) \quad (21)$$

$$A_{12} = \beta_{21} \ (_{is}\ \text{neglected}) \quad (22)$$

$$A_{22} \equiv C = (\beta_{22} + \beta_{222}\,\beta_{22}\,[H^+]^2 + \beta_{224}\beta_{22}\,[H^+]^4 + \beta_{2222}\beta_{222}\,\beta_{22}) \quad (23)$$

$$E_1 \equiv E = [\textstyle\sum^3_{q'} (KH_{1q'})\,(K_W)^{q'}[H^+]^{-q'}] \quad (24)$$

$$E_2 \equiv EE = [\textstyle\sum^2_{q'} (KH_{2q'})\,(K_W)^{q'}[H^+]^{-q'}] \quad (25)$$

Now, in our case: $x \equiv [UO_2{}^{2+}]$ and $y \equiv [HCit^{3-}]$, therefore Eqs. (13-17) lead to:

$$C°_L = x\,[Ay + 2A_{21}y^2] + 2x^2Cy^2 + Dy \quad (26)$$

$$C°_M = x\,[1 + Ay + A_{21}y^2 + E] + 2x^2[EE + Cy^2] \quad (27)$$

$$\Delta C° = (C°_L - C°_M) = Dy - x[1 - A_{21}y^2 + E] - 2x^2EE \quad (28)$$

The variables x and y which are the solutions of Eqs. (26 – 27), depend on the pH of the medium via the expressions of the parameters A, A_{21}, C, D and E, EE. On the other hand, for a given total concentrations $C°_M$ and $C°_L$ and for a given pH, the knowledge of x and y allows us to calculate the fraction in % of the different species in solution and, therefore, to obtain the corresponding diagram of speciation:

$$\%[M_pL_n] = 100.(C°_M)^{-1}\beta_{pn}\,[x]^p[y]^n \quad (29)$$

$$\%[M_pL_nH_m] = 100.(C°_M)^{-1}\beta_{pnm}\,\beta_{pn}\,[x]^p[y]^n \quad (30)$$

$$[H^+]^m \quad \%[M_pL_nH_m(OH)_q] = 100.(C°_M)^{-1}\beta_{pnmq}\,\beta_{pnm}\,\beta_{pn}\,[x]^p[y]^n\,[H^+]^m[H^+]^{-q} \quad (31)$$

$$\%[M_p(OH)_{q'}] = 100.(C°_M)^{-1}(KH_{pq'})\,[OH^-]^{q'}[x]^p \quad (32)$$

V 5. RESOLUTION OF THE EQUATIONS OF CONSERVATION IN THE CASE OF THE URANIUM COMPLEXATION WITH CITRIC ACID

A. Principle

For a given total concentrations $C°_M$ and $C°_L$ of M and L, the resolution of the system of the conservation equations given above depends on five hydrolysis constants $KH_{1q'}$, three acidity constants $K^a{}_1$ and on ten complexation constants β (see Table 4 and Table 5). According to the literature, these last constants are regrouped in seven "sets" which are summed up in Table 4. Indeed, this table lists different β constants given in the literature [2,3,5,10], or calculated according to their corresponding expressions given in "Table 3". In fact, the examination of this table shows that in reality we have only two different independent sets: "Set III" [2,3,5] and "Set V" [2,10]. Indeed, the five other sets are some particular cases of these two sets obtained by neglecting some $[M_pL_nH_m(OH)_q]$ entities (i.e. by taking their corresponding $\beta_{pnmq} = 0$).

Note also that, in order to calculate the β_{122} constant given in "Set V", we used the K_{22I} constant given in reference [10] corresponding to the equilibrium: $(UO_2)^{2+} + 2[H(HCit)]^{2-} \Leftrightarrow [(UO_2)H_2(HCit)_2]^{2-}$ (See Tables 2 and 3). This K_{22I} constant was in fact rejected by the authors of the cited review [10] for the following reasons: The original reference doesn't mention explicitly the experimental conditions used for the determination of this K_{22I} constant. Moreover, the complex $[(UO_2)H_2(HCit)_2]^{2-}$ has not been reported by any other researcher.

On the other hand, Table 5 gives the first five hydrolysis constants $KH_{1q'}$ [10] and the three acidity constants $K^a{}_1$ defined in paragraph 2.1 [7, 10]. All these constants are common to the different sets.

The resolution of the above system involving Eqs. (20 - 32) is generally achieved by the numerical methods explained in paragraph 3.2. Details are given in Appendix I. However, this system could be resolved analytically if we neglect the formation of the following species: $[(UO_2)(HCit)_2]^{4-}$; $[(UO_2)H_2(HCit)_2]^{2-}$; $[(UO_2)_2(OH)]^{3+}$ and $[(UO_2)_2(OH)_2]^{2+}$ and therefore their corresponding constants: (β_{12}), (β_{122}), KH_{21} and KH_{22}. In this approximation, both analytical and numerical calculations lead to identical speciation diagrams. The main advantage of the analytical method consists in the fact that we can resolve the system of Eqs. (20-28) by a Microsoft Office Excel program in order to calculate x and y for different pH and therefore to obtain automatically the graphs of the corresponding speciation diagram: i.e. the % [species] in function of the pH. Details of the analytical resolution are given in Appendix II. It is important to mention that both analytical and numerical calculations must verify the following mass conservation conditions for (UO_2) and (HCit):

$$\textstyle\sum_p\sum_n\sum_m\sum_q p(\%[M_pL_nH_m(OH)_q]) = 100 \quad (31)$$

$$\textstyle\sum_p\sum_n\sum_m\sum_q n(\%[M_pL_nH_m(OH)_q]) = 100 \quad (32)$$

However, analytical and numerical calculations show that, for some ranges of pH, and even if we use a double numerical precision, these conditions are not verified perfectly. The reason for that is the very high sensitivity of the calculations to the parameters used in these pH ranges. This explains why the speciation diagrams presented below are given for different domains of pH between 0 and 14. Indeed, for each figure, we have chosen the best range of pH for which the Eq. (26) and Eq. (27) are verified better than 1%.

This high sensitivity of the calculations to some parameters incited the authors to use their own analytical Excel program and their numerical Basic program, in order to allow a better control of the different stages of calculations. Indeed, this kind of control is not always obvious with the utilization of some usual specific software.

Note finally that ionic strength corrections can be ignored in a first approximation. Indeed more precise numerical calculations on the basis of the self consistent procedure led to the following conclusion: considering the uncertainties on the different constants used in "Set III", "Set IV" and "Set V", the improvement of the results by the recurrent method is not always significant. Besides, in our calculations and experiments, the ionic strength I never exceeded 0.02M.

TABLE 4 DIFFERENT "SETS" OF COMPLEXATION CONSTANTS OF URANIUM IN AUEOUS SOLUTION AT 25 ℃

	"Set I_a"	"Set I_b"	"Set I"	"Set II"	"Set III"	"Set IV"	"Set V"
β_{11}	1.0 10^7	1.0 10^7	1.0 10^7	6.3 10^8	1.0 10^7	6.3 10^8	6.3 10^8
β_{111}	0	7.94 10^4	7.94 10^4	21.37	7.94 10^4	21.37	21.37
β_{1111}	0	3.16 10^{-4}	3.16 10^{-4}	4.07 10^{-2}	3.16 10^{-4}	4.07 10^{-2}	4.07 10^{-2}
β_{112}	0	0	1.26 10^6	1.99 10^4	1.26 10^6	1.99 10^4	1.99 10^4
β_{12}	0	0	0	0	1.0 10^{11}	1.0 10^{11}	1.0 10^{11}
β_{122}	0	0	0	0	0	0	1.0 10^{12} ?
β_{22}	1.0 10^{18}	1.0 10^{18}	1.0 10^{18}	7.94 10^{18}	1.0 10^{18}	7.94 10^{18}	7.94 10^{18}
β_{222}	1	1	1	1	1	1	1
β_{2222}	0	6.3 10^2	6.3 10^2	79.43	6.3 10^2	79.43	79.43
β_{224}	0	0	3.16 10^{11}	3.89 10^{10}	3.16 10^{11}	3.89 10^{10}	3.89 10^{10}

TABLE 5 HYDROLYSIS CONSTANTS KH1Q' AND ACIDITY CONSTANTS KA L AT 25 ℃

KH_{11}	KH_{12}	KH_{13}	KH_{21}	KH_{22}
3.98 10^8	1.99 10^{16}	5.01 10^{21}	1.99 10^{11}	2.51 10^{22}
K^a_1	K^a_2	K^a_3		
7.94 10^5	1.99 10^{10}	1.99 10^{13}		

B. Results in Particular Cases

For a given concentration ratio, $R_c = C°_M / C°_L$, the analytical method allows us to study easily the *sensitivity* of the diagram to the different constants. We used three concentration ratios: $R_c = 0.025$, $R_c = 1$ and $R_c = 2$. Results are summarized in "Figs.1 to 11". Each figure corresponds to a given "set" of constants and to a given ratio R_c.

1) Results Relative to "Set I" Constants in Aqueous Solution at 25 ℃

We have first used both analytical and numerical methods to calculate the uranyl speciation diagram according to the "Set I_a" data given in Table 4 (see Fig. 1). This calculation corresponds to the simplest case for which we neglected both protonation and hydrolysis of M_pL_n entities. Indeed, "Set Ia" differs from "Set I" by the fact that, in this case, all β_{pnm} and β_{pnmq} are ignored. We have also neglected the formation of species $[(UO_2)_2(OH)]^{3+}$, $[(UO_2)_2(OH)_2]^{2+}$, $[(UO_2)(H\ Cit)_2]^{4-}$ and $[(UO_2)H_2(HCit)_2]^{2-}$ (i.e. $KH_{21} = KH_{22} = \beta_{12} = \beta_{122} = 0$).

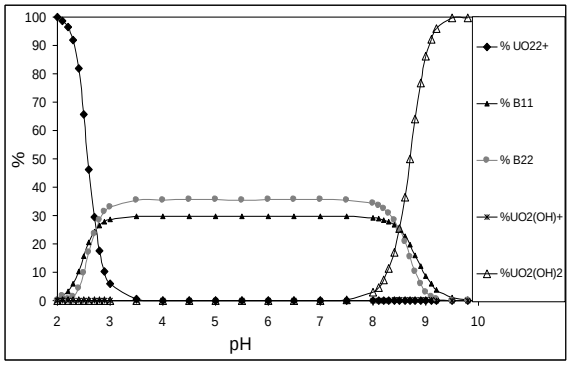

Fig. 1 Speciation diagram of UO_2^{2+} (4.10^{-4}M)) in aqueous $HCit^{3-}$ (2.10^{-2}M) at 25 ℃ with "Set Ia" constants

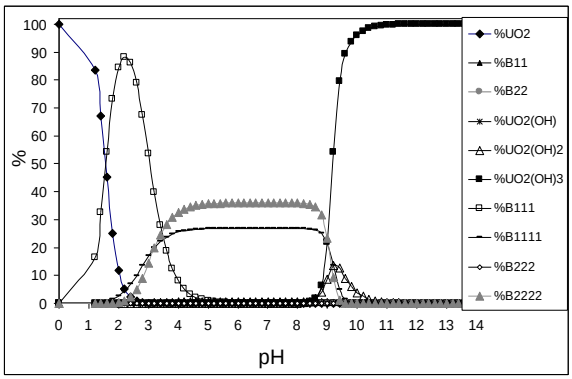

Fig. 2 Speciation diagram of UO_2^{2+} (5.10^{-4}M) in aqueous $HCit^{3-}$ (2.10^{-2}M) at 25 ℃, with "Set Ib" constants and ($\beta112 = \beta224 = 0$)

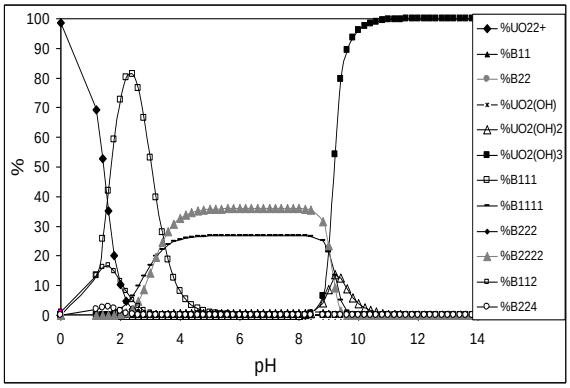

Fig. 3 Speciation diagram of UO_2^{2+} (5.10^{-4}M)) in aqueous $HCit^{3-}$ (2.10^{-2}M) at 25 ℃, with "Set I" constants and ($\beta112 > 0$, $\beta224 > 0$)

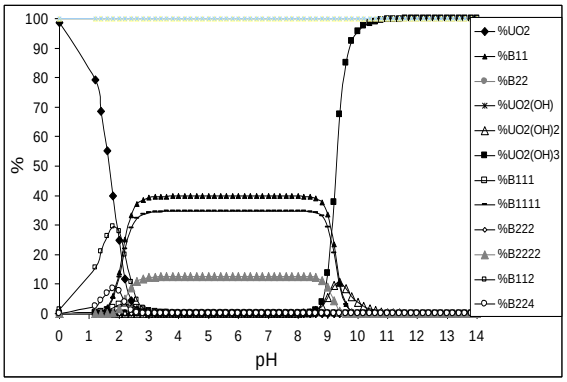

Fig. 4 Speciation diagram of UO_2^{2+} (5.10^{-4}M) in aqueous $HCit^{3-}$ (2.10^{-2}M) at 25 ℃, with "Set II" constants and ($\beta112 > 0$, $\beta224 > 0$)

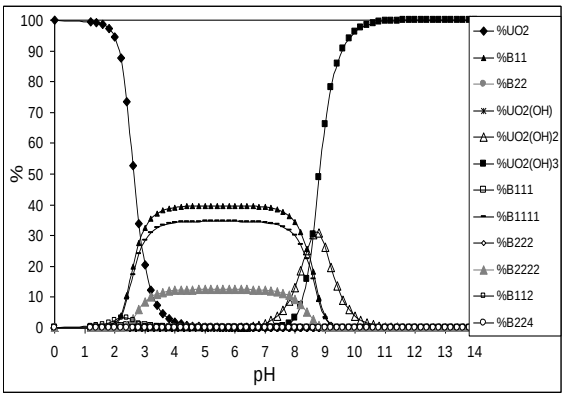

Fig. 5 Speciation diagram of UO_2^{2+} (5.10^{-3}M) in aqueous $HCit^{3-}$ (5.10^{-4}M) at 25 ℃, with "Set II" constants and ($\beta 112 > 0$, $\beta 224 > 0$)

In the second step, we replaced "Set I_a" by "Set I_b" in order to take into account the protonation and the hydrolysis of the complexes $[(UO_2)(HCit)]^-$ and $[(UO_2)_2(HCit)_2]^{2-}$; we thus obtained the diagram reported in Fig. 2. Comparison between Fig. 1 and Fig. 2 shows that, in the pH range: 3 < pH < 9, the two diagrams are similar. In both figures we observe two plateaus of which the levels are around 35% and 25%. The main difference consists in the fact that, in the case of Fig. 1 with "Set I_a", they correspond respectively to $[(UO_2)_2(HCit)_2]^{2-}$ (β_{22}) and $[(UO_2)(HCit)]^-$ (β_{11}) species, whereas in Fig. 2 with "Set I_b", they correspond respectively to the protonated and to the hydrolysed species: $[(UO_2)_2H_2(HCit)_2(OH)_2]^{2-}$ (β_{2222}) and $[(UO_2)H(HCit)(OH)]^-$ (β_{1111}). Besides, around pH ≈2, we observe in (Fig. 2) the apparition of a peak corresponding to a maximum of protonation of type $[(UO_2)H(HCit)]$ (β_{111}).

In the third step, we replaced "Set I_b" by "Set I" in order to take into account the presence of the two species $[MLH_2]$ and $[M_2L_2H_4]$ ($\beta_{112} > 0$; $\beta_{224} > 0$). The corresponding diagram for: $C°_M = 5.0\ 10^{-4}$M and $C°_L = 2.0\ 10^{-2}$ M ($R_c << 1$), is given in Fig. 3. The comparison between Fig. 2 and Fig. 3 shows that the two above-cited species don't modify the shape of the diagram qualitatively and quantitatively. The small difference consists in the apparition (in the region: 0 < pH < 3) of two bell-shaped peaks, with a respectively heights of about 15% and 1.5% (at pH ≈ 1.5) corresponding to $[MLH_2]$ and $[M_2L_2H_4]$ species. Except this small difference, the two figures show:

The % $[UO_2^+]$ decreases from 100% at (pH ≈ 0) to 0% at (pH ≈ 2.5).

The % [MLH] varies as a bell-shaped curve (in the region: 0 < pH < 5); the height of its maximum is of about 85 % at (pH ≈ 2.5). Note that this peak is (in our case) non observable by capillary electrophoresis method because $[UO_2H_2Cit]$ is a neutral species.

In the pH range: 4 < pH < 8.5, both %[MLH(OH)] and $\%[M_2L_2H_2(OH)_2]$ are constants (two plateaus) respectively equal to 25% and 35%. At pH ≈ 3.25 and pH ≈ 9, the percentage of these two species are sensibly equal: $\%[MLH(OH)] = \%[M_2L_2H_2(OH)_2] \approx 20\%$.

The $\%[M(OH)_3]$ presents a gap of height of about 95%, in the region: 8.5 < pH < 9.5

The $\%[M(OH)_2]$ is a bell-shaped curve (in the pH range: 8.5 < pH < 10.5); the height of its corresponding peak is about 13 % at pH ≈ 9.3.

In summary, according to "Set I" constants and for $R_c << 1$, we observe quantitatively only 8 species in the pH range: 0 < pH < 14. Notice however that, only the two anionic complexes: $[(UO_2)\ H(HCit)(OH)]^-$ and $[(UO_2)_2\ H_2(HCit)_2\ (OH)_2]^{2-}$, are observable by the capillary electrophoresis method in the pH range under consideration. Within the limits of experimental precision, these two species are observable for 3 ≤ pH ≤ 9.

2) Results Relatively to "Set II" Constants in Aqueous Solution at 25 ℃

The difference between "Set I" and "Set II" consists essentially in the fact that β_{11} (Set I) < β_{11}(Set II) and β_{111}(Set II) << β_{111}(Set I). The corresponding diagram, for $C°_M = 5.0.10^{-4}$; $C°_L = 2.0\ 10^{-2}$ ($R_c << 1$), is given in Fig. 4 which shows that:

The peak of the bell-shaped curve (in the region 0 < pH < 5 of Fig.3), corresponding to %[MLH], becomes negligible. Indeed, its height is only of about 3 % at pH ≈ 2.5.

A third "plateau" appears, in pH range: 2.5 < pH < 9, with a height of about 40 %, which corresponds to the [ML] specie (it is the main difference between "Set I" and "Set II").

In the same pH range: 2.5 < pH < 9, and by comparison to Fig. 3, we observe an inversion of the plateaus corresponding to the species [MLH(OH)] (35%) and to the species $[M_2L_2H_2(OH)_2]$ (10%) rather than the corresponding percentages: 25% and 35% respectively observed in the case of Fig. 3 relatively to "Set I".

Except these differences, Fig. 4 is comparable to Fig. 3. Notice, however, that in the present case (Fig. 4), the intensities of the peaks corresponding to the species $[MLH_2]$ (30%) and $[M_2L_2H_4]$ (8%) are the double of those of Fig. 2 relatively to "Set Ib"

In summary, with "Set II" constants and $R_c << 1$, we again observe quantitatively 8 species in the pH range: 0 < pH < 14. However, in contrast with "set I", three anionic complexes: $[(UO_2)(HCit)]^-$, $[(UO_2)H(HCit)(OH)]^-$ and $[(UO_2)_2\ H_2(HCit)_2\ (OH)_2]^{2-}$, are observable by capillary electrophoresis, for 3 ≤ pH ≤ 9, within the limits of experimental precision.

3) Concentration Effect at 25 ℃

In order to study the sensitivity of the speciation diagram to the concentration ratio, R_c , in the case of the "Set II" constants, we established the diagrams presented in Fig. 5 and Fig. 6 respectively:

$C°_M = 5.0\ 10^{-4}$; $C°_L = 5.0\ 10^{-4} \Leftrightarrow R_c = 1$, (given in Fig. 5).

$C°_M = 1.0\ 10^{-3}$; $C°_L = 5.0\ 10^{-4} \Leftrightarrow R_c = 2$, (given in Fig. 6).

Fig. 5 shows that, when the solution is equimolar in $[(UO_2)]$ and [(HCit)], peaks corresponding to species [MLH], $[MLH_2]$ and $[M_2L_2H_4]$ are negligible (< 2%). In contrast, the height of the $[M(OH)_2]$ peak (in the region 7 < pH < 10) is now of about 30 % at pH ≈ 9.

However, and as in the case of Fig. 4 ($R_c<<1$), Fig. 5 shows three plateaus corresponding to the % of the species: [ML], [MLH(OH)] and $[M_2L_2H_2(OH)_2]$, of heights respectively equal to 40%, 35% and 10%, in the pH range: 3 < pH < 8. Notice also that the two gaps corresponding to the species $[(UO_2)]^{2+}$ and $[(UO_2)\ (OH)_3]^-$ (for $R_c = 1$) are comparable to those of Fig. 4 (for $R_c <<1$).

In conclusion, we can say that, for R_c=1, the species ($[(UO_2)(HCit)]^-$, $[(UO_2)H(HCit)(OH)]^-$ and $[(UO_2)_2H_2(HCit)_2(OH)_2]^{2-}$) are observable by capillary electrophoresis, in the pH range: $3 \le pH \le 8$.

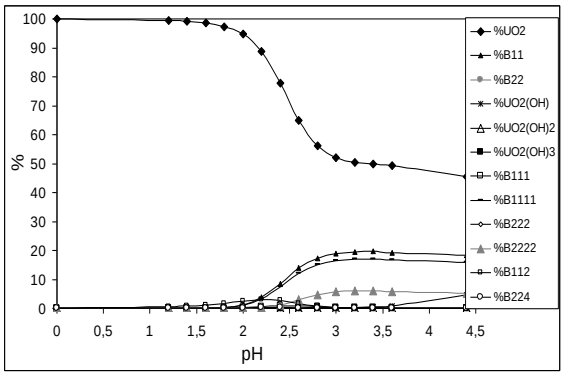

Fig. 6 Speciation diagram of UO_2^{2+} (10^{-3}M) in aqueous $HCit^{3-}$ (5.10^{-4}M) at 25 ℃, with "Set II" constants and ($\beta112 > 0$, $\beta224 > 0$)

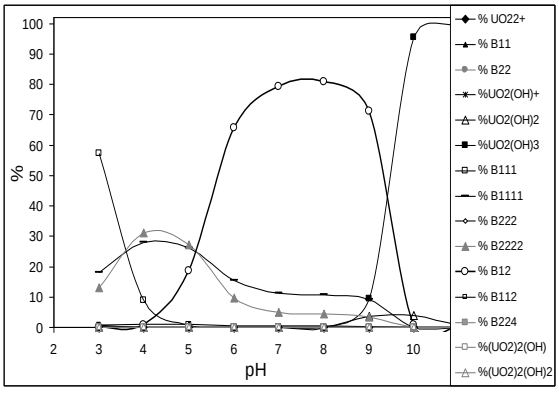

Fig. 7 Speciation diagram of UO_2^{2+} (4.10^{-4}M)) in aqueous $HCit^{3-}$ (2.10^{-2}M) at 25 ℃ with "Set III" constants; $\beta112 = 0$

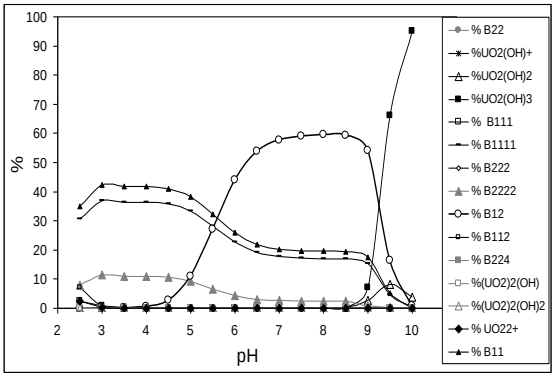

Fig. 8 Speciation diagram of UO_2^{2+} (4.10^{-4}M)) in aqueous $HCit^{3-}$ (2.10^{-2}M) at 25 ℃ with "Set IV" constants; $\beta112 = 0$

On the other hand, Fig. 6 (for $R_c = 2$) shows that the excess of $[(UO_2)]^{2+}$ ions changes appreciably the speciation diagram in the sense that the respective heights of the plateaus: [ML], [MLH(OH)] and $[M_2L_2H_2(OH)_2]$ are decreased, in the pH range: $3 < pH < 5$, toward: 15%, 10% and 5%, respectively. Notice also that the variation with pH of the percentage of the species $[(UO_2)]^{2+}$ is now completely different, by comparison to Figs. 4, 5. In particular, this percentage remains sensibly constant equal to 45 % in the pH range: $3 < pH < 5$ (for $R_c = 1$). Nevertheless, we can say that, for R_c=2, the species $[(UO_2)(HCit)]^-$ and $[(UO_2)H(HCit)(OH)]^-$ remain observable by capillary electrophoresis, in the pH range: $3 \le pH \le 5$. However, and within the limits of the experimental precision, this fact is less true for $[(UO_2)_2H_2(HCit)_2(OH)_2]^{2-}$ species.

C. Results in the General Case at 25 ℃

In the general case, and in addition to the previous entities, we have taken into account the formation of the following species: $[(UO_2)(HCit)_2]^{4-}$: (β_{12}), $[(UO_2)_2(OH)]^{3+}$: (KH_{21}), $[(UO_2)_2(OH)_2]^{2+}$: (KH_{22}). Their corresponding constants: (β_{12}), (KH_{21}) and (KH_{22}) are given in Table 4 ("Set III" ≡ "Set I" + β_{12} or "Set IV" ≡ "Set II" + β_{12}) and in Table 5. The questionable case of the specie $[(UO_2)H_2(HCit)_2]^{2-}$: (β_{122}) will be analyzed at the end of this paragraph.

The numerical result corresponding to "Set III" is represented in Fig. 7. Comparison with Fig. 3 ("Set I") shows that except for the two pH ranges: $3 < pH < 5$ and $9 < pH < 11$, the two diagrams are completely different. Indeed, with "Set III" constants and for $pH > 5$, the percentages of both species: $[(UO_2)H(HCit)(OH)]^-$: (β_{1111}) and $[(UO_2)_2H_2(HCit)_2(OH)_2]^{2-}$: ($\beta_{2222}$) decrease with pH from 30% to respectively: 10% and 5% in the pH range: $6 < pH < 9$. This decrease is offset by the apparition in the same pH range of an important "plateau" of about 80 % height, corresponding to the specie $[(UO_2)(HCit)_2]^{4-}$: (β_{12}).

Now if we replace "Set III" by "Set IV", so that β_{11}(Set III) < β_{11}(Set IV) and β_{111}(Set IV) << β_{111}(Set III) (by analogy to the transformation of "Set I" into "Set II"), we obtain the diagram given by Fig. 8. Comparison of Fig. 8 with the previously Fig. 7 indicates the apparition with a relatively important percentage of the specie $[(UO_2)(HCit)]^-$ in addition to the species: $[(UO_2)H(HCit)(OH)]^-$ and $[(UO_2)_2 H_2(HCit)_2 (OH)_2]^{2-}$ (by analogy to the comparison between Fig. 4 ("Set II") and Fig. 3 ("Set I")). Consequently, the height of the "plateau" corresponding to the specie $[(UO_2)(HCit)_2]^{4-}$ is now of about 60 % rather than 80%.

In conclusion, we can say that numerical calculation for $R_c << 1$ predicts that the species $[(UO_2)(HCit)]^-$, $[(UO_2)H(HCit)(OH)]^-$ and $[(UO_2)_2H_2(HCit)_2(OH)_2]^{2-}$ should be observable by capillary electrophoresis in the region: $3 \le pH \le 5$, even if we take into account of the species $[(UO_2)(HCit)_2]^{4-}$ which become observable only for pH>5 and this independently of the choice of the literature values of $\beta_{11}$and β_{111} for the calculation. Indeed, $\beta_{11}$and β_{111} , influence rather the relative peak intensities of the three observable entities.

If in addition we suppose the formation of the specie $[(UO_2)H_2(HCit)_2]^{2-}$ in conformity with the "Set V" ≡ ["Set IV" with: $\beta_{122} = 1.0\ 10^{12}$] we therefore obtain the diagram given in Fig. 9 calculated for $R_c << 1$. This diagram shows clearly that the introduction of the β_{122} constant provokes the complete disappearance of all the species $[(UO_2)(HCit)]^-$, $[(UO_2)H(HCit)(OH)]^-$ and $[(UO_2)_2H_2(HCit)_2(OH)_2]^{2-}$ in the pH range: $2 < pH < 5$. This disappearance is compensated (up to 100% !) by the species$[(UO_2)H_2(HCit)_2]^{2-}$. For pH>5, Fig. 9 remains quite similar to Fig. 8. Thus, according to the above hypothesis ($\beta_{122} \neq 0$), numerical calculations show that for $R_c << 1$, $[(UO_2)H_2(HCit)_2]^{2-}$ is the only observable specie in the pH range: $3 \le pH \le 5$. We will see that this conclusion is not verified by the capillary electrophoresis experiments.

1) Concentration Effect in the General Case at 25 ℃

In order to study, in the general case characterized by "Set V" constants, the sensitivity of the speciation diagram to the concentration ratio R_c, we have established the following diagrams given by Fig 10 and Fig. 11, respectively for:

$C°_M = 5.0\ 10^{-4}$; $C°_L = 5.0\ 10^{-4} \Leftrightarrow R_c = 1.$

$C°_M = 1.0\ 10^{-3}$; $C°_L = 5.0\ 10^{-4} \Leftrightarrow R_c = 2.$

Comparison of Fig 10 (with: $\beta_{12} > 0$, $\beta_{122} > 0$) with Fig. 5 ($\beta_{12} = 0$, $\beta_{122} = 0$) shows that the formation of species $[(UO_2)(HCit)_2]^{4-}$ has no significant influence on the diagram, and that the influence of $[(UO_2)H_2(HCit)_2]^{2-}$ species is also negligible by comparison with Fig. 9 ($R_c << 1$). Indeed, the height of their corresponding bell-shaped peak in Fig. 10 doesn't exceed 7% in the pH range: 2 < pH < 4.

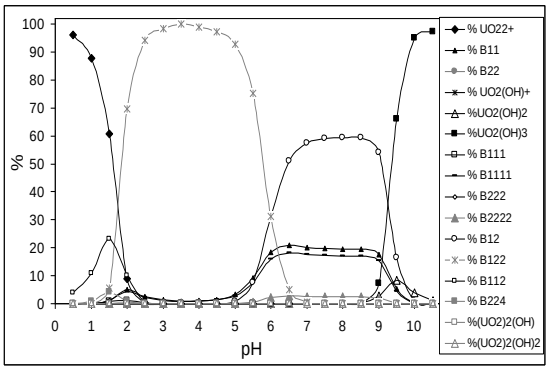

Fig. 9 Speciation diagram of UO_2^{2+} (4.10^{-4}M)) in aqueous $HCit^{3-}$ (2.10^{-2}M) at 25 °C with "Set V" constants; β112 > 0

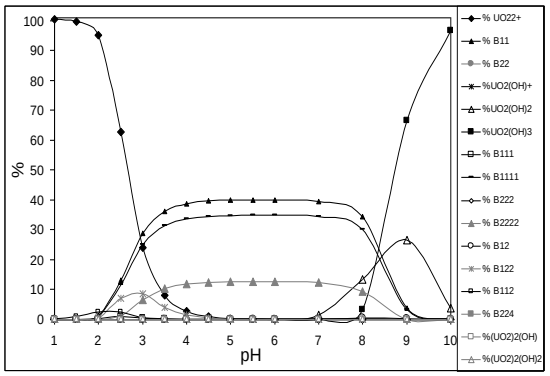

Fig. 10 Speciation diagram of UO_2^{2+} (5.10^{-4}M) in aqueous $HCit^{3-}$ (5.10^{-4}M) at 25 °C with "Set V" constants; β112 > 0

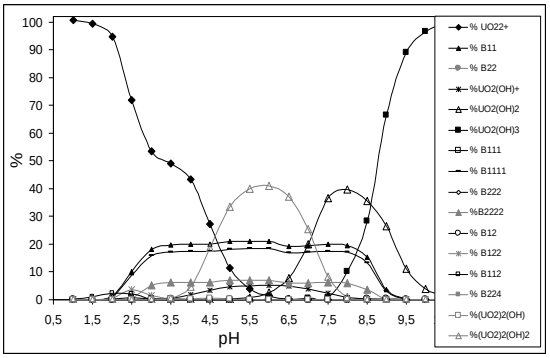

Fig. 11 Speciation diagram of UO_2^{2+} (10^{-3}M) in aqueous $HCit^{3-}$ (5.10^{-4}M) at 25 °C with "Set V" constants; β112 > 0

Note also that the two gaps corresponding to both $[(UO_2)]^{2+}$ and $[(UO_2)(OH)_3]^-$ species, for $R_c = 1$, are also comparable to those of Fig. 5 (R_c =1).

In the same manner, comparison of Fig. 11 ($R_c = 2$, $\beta_{12} > 0$, $\beta_{122} > 0$) with Fig. 6 (relative to "Set II": $\beta_{12} = 0$, $\beta_{122} = 0$ and $R_c = 2$), shows that the formation of the two species $[(UO_2)H_2(HCit)_2]^{2-}$ and $[(UO_2)(HCit)_2]^{4-}$ is always negligible. Indeed, the heights of their corresponding peaks are respectively less or of about 3% in the pH range: 2 < pH < 3. Notice finally that, according to Fig. 11, the relative excess of $(UO_2)^{2+}$ ions (characterized by the ratio: $R_c = 2$), increases the maxima of the bell-shaped peaks relative to the species $[(UO_2)_2(OH)_2]^{2+}$ and $[(UO_2)(OH)_2]$, respectively up to 43% in the pH range: 3 < pH < 8, and to 40% in the pH range: 6 < pH < 10. However, these peaks cannot be observed experimentally in the present case of our experience.

In conclusion, the formation of $[(UO_2)H_2(HCit)_2]^{2-}$: (β_{122}) and $[(UO_2)(HCit)_2]^{4-}$: (β_{12}) species seems to appear with important and constant percentages (respectively: 95% for: 1.5 < pH < 6.5 and 60% for: 4.5 < pH < 10), *only* for low ratios: $R_c << 1$. In contrast, for $R_c \geq 1$, the percentage of $[(UO_2)H_2(HCit)_2]^{2-}$ is ≤ 5%, whereas, the rate of $[(UO_2)(HCit)_2]^{4-}$ remains negligible. This means that, in the range of pH studied experimentally (pH < 5), numerical computations predict the apparition of only one intense peak for dilute solutions in uranium which must disappear with increasing the U (VI) concentration. This prediction is not in agreement with our previous observations [16]. Therefore, the hypothesis of the existence of the $[(UO_2)H_2(HCit)_2]^{2-}$ specie seems unlikely. In contrast, calculations according to: "Set I to Set IV" predict the observation of *three* peaks in the pH range: 2 < pH < 5, corresponding to the $[(UO_2)(HCit)]^-$, $[(UO_2)H(HCit)(OH)]^-$ and $[(UO_2)_2H_2(HCit)_2(OH)_2]^{2-}$ species. However, the importance of the $[(UO_2)(HCit)]^-$ peak depends on the choice of the $\beta_{11}$and β_{111} constants. Notice that according to the reference [10], the most probable species in the pH range: 2 < pH < 5 are rather $[(UO_2)(HCit)]^-$ and $[(UO_2)_2(HCit)_2]^-$ (See Fig. 1 obtained with "Set Ia"). This conclusion is not compatible with the diagrams calculated with the data of the all other sets as long as we assume that the different protonation and hydrolysis reactions have reached their complete chemical equilibrium.

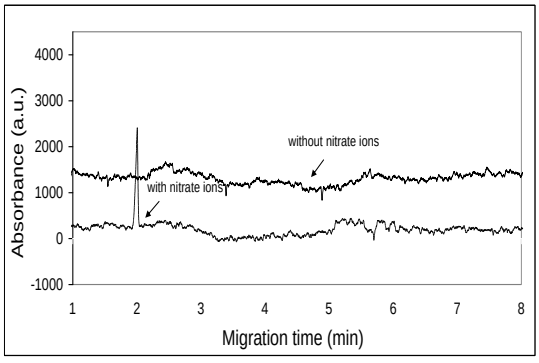

Fig.12 Comparison between electropherograms of sodium citrate buffer solutions at pH=3 containing or not NO_3^- ions

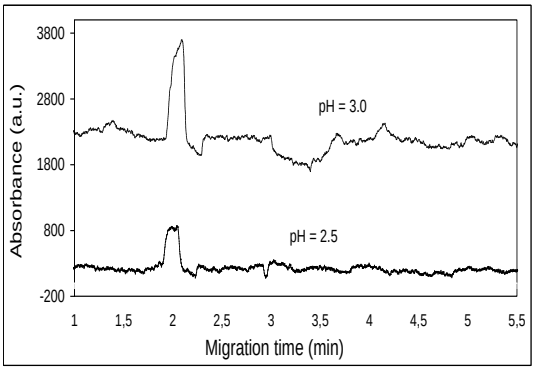

Fig. 13a Electropherograms of 1.10^{-5}M nitrate and 5.10^{-4}M U(VI) in 0.02 M citrate buffer at pH=2.5 and pH=3.0

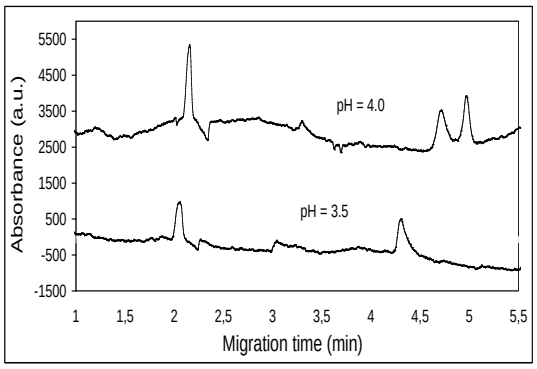

Fig. 13b Electropherograms of 1.10^{-5}M nitrate and 5.10^{-4}M U(VI) in 0,02M citrate buffer at pH=3.5 and pH=4.0

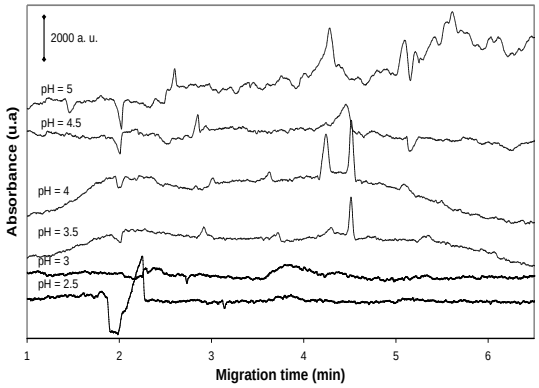

Fig. 14 Electropherograms of 5.10^{-4}M U(VI) in 0.02M citrate buffer at various pH values

VI EXPERIMENTAL

A. Apparatus

The capillary electrophoresis apparatus is a modular system consisting of a Spectraphoresis 100 injector (hydrodynamic mode) coupled with a high voltage (0-30kV) power supply (Prime Vision VIII from Europhor) and a scanning UV-visible detector (Prime Vision IV from Europhor). In the present study, a voltage of 30kV was applied and a fixed wavelength of 200 nm was chosen for the absorbance measurements. The external temperature was maintained equal to 25°C. The acquisition of the electropherograms and the data treatment were performed using the chromatography software BORWIN (JMBS Développements).

Each measurement was repeated two or more times in order to assure the reproducibility condition.

B. Chemicals

All solutions were prepared with deionised water and chemicals of analytical reagent grade. For the sodium citrate buffer solutions, we have used different Fluka solutions for HPCE (210^{-2}M) having pH values between 2.5 and 5.5. The uranyl stock solution (concentrated UO_2 $(ClO_4)_2$) was prepared by dissolving 1g of uranyl nitrate hexahydrate salt, $UO_2(NO_3)_2.6H_2O$ (FLUKA), in 25 ml of concentrated perchloric acid. The resulting mixture was then almost completely evaporated at 150°C in a sand bath and this procedure was repeated several times in order to eliminate all the nitrates. This acidic ($HClO_4$ + UO_2 $(ClO_4)_2$) stock solution was then diluted in order to adjust the uranyl concentration to around 10^{-2}M (the exact concentration was determined by fluorescence spectroscopy).

For each pH value of the citrate buffer, a corresponding sample was prepared by mixing appropriate volumes of diluted uranyl stock solution and sodium citrate buffer solution. The final pH of this sample solution was adjusted by adding a small quantity of NaOH solution (0.1M). The total final volume of the different prepared samples is equal to 1000 µl.

It is important to mention that, before performing any electrophoresis experiment, the sample solutions were kept at rest for at least two days, in order to allow the different reactions of complexation, protonation, and hydrolysis, to reach their complete chemical equilibrium.

C. Procedure

The silica capillary (SUPELCO, 75 µm of internal diameter, 75 cm long), was first conditioned by successive washes with 0.1 NaOH, then by deionised water, and finally by 0.02M sodium citrate buffer solution of a given pH.

The cleanliness of the capillary is checked by a first run using only the buffer solution under study (check of the baseline). The corresponding electropherogram should not present any peak but only a smooth baseline (or noise line).

In order to control the eventual effect of the electroosmotic flow (neglected at low pH values [11]), as well as other experimental fluctuations, which can shift the peak positions of the anionic species under observation, nitrate ions (at very low concentrations) were added to some samples. This anion has already been used in previous works as a reference anion for mobility measurements [12, 13, 16]. Fig. 12 gives an example of such electropherograms obtained at pH = 3 (NO_3^- peak appears around 2 min).

Each run consisted in a hydrodynamic injection of 2n nanoliters during n sec, of a sample solution (uranyl solution in buffer citrate with or without nitrate ions) into the capillary. The corresponding electropherogram was obtained by applying 30 kV during an acquisition time of at least 10 min. Finally, the capillary was carefully rinsed with the buffer under study between two runs and kept filled with deionised water during the night.

D. Results and Discussion

As expected, since citrate ions are absorbing species in the UV domain, the stability of the baseline is very sensitive to the buffer pH value, as can be seen in Figs.13, 14. The background absorbance was observed to increase with pH and strong fluctuations to appear for pH > 4.5. These changes in the level and quality of the baseline can be assigned to an augmentation of the charged citrate ions of the buffer when pH increases. Consequently, the current passing through the capillary increases sharply with pH: (from 20 □ A at pH 2.5~ 3 to 135 □A at pH 5). For these reasons, the best results were obtained, for: 2.5 < pH <4.5 (the reasonable limit, 70 – 75 □A, is reached at pH 4.5). The different results are summarized in the electropherograms presented in "Figs.13a, 13b" and in Fig. 14. All of them were obtained for $C°_L$ = 0.02 M, $C°_M = 5\ 10^{-4}$M and eventually $C°_{NO3-} = 1.10^{-5}$M. They show the existence of three peaks which can be assigned with the anion uranyl species; the most mobile entities are those which present, the low time of migration.

1) Electropherograms for: 2 < pH ≤ 3

According to "Set I" constants (β_{11}, β_{111}, β_{1111}, β_{112}, β_{22}, β_{2222}, β_{224}, KH_{11}, KH_{12}, KH_{13}) or "Set III" ≡ {"Set I" + β_{12}}

(see "Fig.3" or "Fig. 7"), only cationic ($[(UO_2)H_2(HCit)]^+$, $[(UO_2)_2H_4(HCit)_2]^{2+}$) or neutral ($[(UO_2)H(HCit)]$) species, exist for pH < 3. The two anionic species: ($[(UO_2)H(HCit)(OH)]^-$, $[(UO_2)_2H_2(HCit)_2(OH)_2]^{2-}$), are thus expected to appear quantitatively only for pH >3.5. Notice that, according to "Set II" constants (β'_{11}, β'_{111}, β'_{1111}, β'_{112}, β'_{22}, β'_{2222}, β'_{224}, KH_{11}, KH_{12}, KH_{13}) or "Set IV" ≡ {"Set II" + β_{12}} constants (see Fig.4 or Fig. 8), the three anionic species: ($[(UO_2)(HCit)]^-$, $[(UO_2)H(HCit)(OH)]^-$ and $[(UO_2)_2H_2(HCit)_2(OH)_2]^{2-}$) appear also quantitatively, only for pH > 3. These theoretical results are in good agreement with the fact that, for pH = 2.5 and pH = 3, the corresponding electropherograms do not point out any peak associated with anionic uranyl species. The only apparent peak shown in Fig. 13a, with a migration time t ≈ 2 min, is due to the added nitrate ions.

2) Electropherograms for: 3 < pH < 5

In contrast, for buffer pH values around 4, the corresponding electropherograms show three separate peaks at migration times of ≈ 3.2 min, t ≈ 4.7 min and t ≈ 5 min (see Fig. 13b, 14). Owing to our theoretical results, these peaks could be assigned to the three following species: $[(UO_2)_2H_2(HCit)_2(OH)_2]^{2-}$, $[(UO_2)H(HCit)(OH)]^-$ and $[(UO_2)(HCit)]^-$.

Their electrophoretic mobility, u_i, can be derived from the one of NO_3^-: u_{NO3}, by applying the following expression:

$$u_i = u_{NO3}^- + (d\ L/U)\ (1/t_{Mi} - 1/t_{NO3}^-) \qquad (33)$$

where u_{NO3} is the ionic mobility of NO_3^- ($7{,}4\ 10^{-4}$ $cm^2\ V^{-1}\ s^{-1}$); U is the applied voltage (30 000 V); L is the capillary length (75cm) and d, the length from the capillary inlet to the detector (35 cm). The parameters: t_{Mi} and t_{NO3} are respectively the times taken by the ionic "i" specie and by the NO_3^- specie to reach the detector [12].

TABLE 6 ELECTROPHORETIC MOBILITIES, UI, CORRESPINDING TO THE PEAKS OBSERVED IN FIG. 13B (NO3- BEING TAKEN AS REFERENCE)

	pH = 3.5		pH = 4.0	
	t(migration) (sec)	$10^4\ u_i$ ($cm^2\ V^{-1}\ s^{-1}$)	t(migration) (sec)	$10^4\ u_i$ ($cm^2\ V^{-1}\ s^{-1}$)
NO_3^-	122.2	(7.4)	128	(7.4)
species 1	180.9	5.08	195	5.06
specie 2	256	3.66	279.5	3.73
specie 3			294.8	3.54

The calculation leads to the following electrophoretic mobility values: $5.1\ 10^{-4}$, $3.7\ 10^{-4}$ and $3.5\ 10^{-4}$ $cm^2\ V^{-1}\ s^{-1}$ (see Table 6), corresponding to the three uranyl complex forms detected in Fig. 13b. However, the exact correspondence between each of these values and the above cited anionic species is not a priori evident. Nevertheless, the ionic mobilities of monomer species are generally assumed to be approximately proportional to their charge over size ratio [13]. Indeed, according to the Nernst-Einstein relation: $u_iD_i^{-1} = (Z_ie)(kT)^{-1}$ and Stokes-Einstein relation: $D_i = kT(6\pi\eta R_i)^{-1}$, where: D_i is the self diffusion coefficient, kT is the thermal energy, η is the viscosity and Z_ie, R_i are the charge and the radius of the considered "i" specie, the expression of the mobility is therefore: $u_i = (Z_ie)/(6\pi\eta R_i)$. Consequently, we have attempted to make the following qualitative predictions on the basis of the different structures attributed by recent literature to the three complexes under consideration:

$[(UO_2)H(HCit)(OH)]^-$ and $[(UO_2)(HCit)]^-$ they have the same charge and similar radii; therefore, they should have near mobility values. The two peaks observed at pH > 3.5 at migration time t ≈ 4.8 min, and characterized by a weak separation and a comparable height(see Fig. 13b, 14), can thus be attributed to these two species. Indeed, if we assume the validity of the "Set II" constants, these two species are also expected to have close complexation rates (or %), in accordance with the theoretical predictions: 40% and 35%, for respectively $[(UO_2)(HCit)]^-$ and $[(UO_2)H(HCit)(OH)]^-$ (see Figs. 4, 8). We can note, however, that at pH = 3.5, and in contrast with pH =4, only one of the two close peaks appears clearly on the corresponding electropherograms (the second peak could only be guessed on the electropherogram of Fig. 14). Comparison between Fig. 13a and Fig. 13b shows that the percentage of the two above cited species increases from pH ≈2.5 to pH 4 with a gap at pH ≈ 3. This tendency is reflected in the diagrams given in Figs. 4, 8 but with a gap at pH ≈ 2.5.

The $[(UO_2)_2H_2(HCit)_2(OH)_2]^{2-}$ the complexion has a double negative charge (Z_i = -2) and it exhibits three possible conformations [14]: two of them are rather spherical characterized by a large radius R_i and therefore by a weak diffusion coefficient: D_i; In contrast, the third most probable conformation, is a cylindrical chain presenting a weak viscous friction and therefore, a large mobility u_i [15]. However, since its corresponding complexation rate is about 10%, (according to our theoretical calculations: Figs. 4, 8), its relative electrophoretic peak should be weak. This fact is confirmed by the electropherograms performed at pH 3.5, pH4 and pH 4.5 after a migration time of about: t ≈ 3.0-3.5 min.

Note moreover that, for pH ≥ 4.5, this peak (at t ≈ 3 min) is always observable, whereas the other two peaks are, more or less hidden by the noise of the baseline (see Fig.14). On the other hand, according to our calculation using "Set II" constants, the increasing of the U(VI) concentration (i.e. the ratio Rc), will not give more information concerning these three species since their percentages decrease with increasing the ratio Rc.

It is interesting to underline at this stage, and more particularly for the speciation measurements under consideration, the interest of the capillary electrophoresis method by comparison to some other analytical methods: the latter ones are rather sensitive to the coordination state of U(VI), (for example, because of the variation of the U-O distance with pH). It ensues that these techniques cannot in general distinguish between protonated and non- protonated complexes: M_1L_1, $M_1L_1H_1$, $M_1L_1H_2$, M_2L_2, $M_2L_2H_2$, and $M_2L_2H_4$, as well as between hydrolyzed and non-hydrolyzed complexes: (for example: $M_1L_1H_1(OH)_1$ or $M_2L_2H_2(OH)_2$). In other terms, and for the present study, they could not inform us sufficiently on the protonation state nor on the hydrolysis state of M ≡ U(VI). On the other hand, the capillary electrophoresis method, which is very sensitive to both the charge Z_ie and/or the size of the species, allows the separation of the different anionic complexes expected to be formed on the base of their relative mobility.

VII CONCLUSION

In order to complete more deeply our previous work [16] in selecting the more appropriate complexation constants among those published by the literature, and following the controversy concerning the processes of protonation and the

hydrolysis of the uranyl-citrate species, we undertook to compare our new uranyl-citrate speciation diagrams calculated analytically or numerically with experimental results obtained by the capillary electrophoresis method, in dilute citrate aqueous solutions (0.02M) at 25 ℃ and for: 2.5 < pH < 5.

Calculations show 16 possible $[M_pL_nH_m(OH)_q]$ entities, with: $M \equiv (UO_2)^{2+}$, $L \equiv (HCit)^{3-}$. For $R_c = 0.02$, cationic ($[(UO_2)H_2(HCit)]^+$, $[(UO_2)_2H_4(HCit)_2]^{2+}$) or neutral ($[(UO_2)H(HCit)]$) protonated U(VI)-citrate-complexes appear for pH < 3. Using "Set II" constants, three anionic ($[(UO_2)(HCit)]^-$,$[(UO_2)H(HCit)(OH)]^-$, $[(UO_2)_2\ H_2(HCit)_2\ (OH)_2]^{2-}$) species appear mainly for: 3 < pH < 5 with respectively rates of about: 40%, 35% and 10%. For: 5 < pH < 9, these proportions decrease of half (20%, 15% and 5%) if we assume the formation of the $[(UO_2)(HCit)_2]^{4-}$ specie. For pH > 9, the specie $[(UO_2)(OH)_3]^-$ is predominant. Notice that if we assume the existence of the $[(UO_2)H_2(HCit)_2]^{2-}$ specie (reported by only one reference), the speciation diagram is then completely modified in the range: 1.5 < pH < 6, since its percentage in this domain is evaluated to 95%. However, for $R_c \geq 1$, both $[(UO_2)(HCit)_2]^{4-}$ and $[(UO_2)H_2(HCit)_2]^{2-}$ species become negligible; consequently, the respective proportions of the three $[(UO_2)(HCit)]^-$, $[(UO_2)H(HCit)(OH)]^-$, $[(UO_2)_2\ H_2(HCit)_2(OH)_2]^{2-}$ species become constant (3 plateaus) in the region: 3 < pH < 8. For: $R_c = 1$, these percentages are about: 35%, 30% and 10%. For: $R_c = 2$, they decrease to about: 20%, 17% and 5% because of the predominance of the free $(UO_2)^{2+}$ ion for pH < 4, and also due to the apparition of the hydrolyzed ions: $[(UO_2)_2(OH)_2]^{2+}$ for 4.5 < pH < 7 and $[(UO_2)(OH)_2]$ for 7 < pH < 9. It is interesting to notice that less recent constant data ("Set Ib"), lead to the same results, except that the specie $[(UO_2)(HCit)]^-$ is substituted by the neutral specie $[(UO_2)H(HCit)]$, which appears only for pH < 3.5.

The application of the capillary electrophoresis technique to the study of the uranyl-citrate speciation in dilute acidic aqueous solutions for: (2.5 < pH < 5), confirms qualitatively our theoretical predictions. Indeed, the corresponding electropherograms, show two close electrophoretic peaks (or nearly superimposed) of comparable heights and a third small peak. We could assign the two first peaks to $[(UO_2)(HCit)]^-$ and $[(UO_2)H(HCit)(OH)]^-$ species, while the third peak represents the $[(UO_2)_2H_2(HCit)_2(OH)_2]^{2-}$ species. The corresponding proportions are about 40%, 35% and 10% at pH 4. On the other hand, our experimental results invalidate, as expected, the existence of the $[(UO_2)H_2(HCit)_2]^{2-}$ specie (which, in principle, should appear with a rate of about 95% for 1.5 < pH < 6.5 and for R_c<<1). Moreover, the observation of the $[(UO_2)(HCit)_2]^{4-}$ specie in the region of pH > 4.5, seems to be screened by the noise effect. Notice however that, this numerical speciation analysis is based on the assumption: that all the protonated and hydrolyzed species have reached their complete chemical equilibrium. Nevertheless, the present study enabled us to emphasize the capacity of the capillary electrophoresis technique to separate (at least qualitatively) different ionic complexes and to specify their degrees of protonation and hydrolysis even out of their equilibrium states. Indeed, it was particularly possible for us to prove the reliability of the processes of protonation and hydrolysis of both the monomer and the dimer: $[(UO_2)(HCit)]^-$, $[(UO_2)_2(HCit)_2]^{2-}$ in the following forms: $[(UO_2)\ H(HCit)\ (OH)]^-$ and $[(UO_2)_2H_2(HCit)_2(OH)_2]^{2-}$. This conclusion opens new fundamental prospects in the aim of explaining (in terms of competition between ligands, OH^- and H_2O [17]) how the complexation of a metal cation similar to UO_2^{2+} (whose hydrolysis generally occurs at relatively elevated pH) facilitates in certain cases the process of its hydrolysis at a lower pH.

ACKNOWLEDGMENTS

The authors would like to acknowledge the financial and the technical supports provided partly, by the General Direction of Scientific Research of Tunisia (DGRST), the National Centre of Scientific Research of France (CNRS) and the Institute of Nuclear Physics, IN2P3-CNRSof Orsay.

APPENDIX I NUMERICAL RESOLUTION OF THE EQUATIONS OF CONSERVATION

In the general case of: $\beta_{12} > 0$ and $\beta_{122} > 0$, the corresponding system of conservation equations is given by Eqs. (26-28) with: $x \equiv [UO_2^{2+}]$ and $y \equiv [HCit^{3-}]$, therefore:

$$y = 0.5[-D + \Delta^{1/2}](xA_{21})^{-1} \quad (I.1)$$

with: $\Delta = D^2 + 4(xA_{21})[\Delta C^\circ + x(1+E) + 2x^2EE]$ (I.2)

$$\Delta C^\circ = (C^\circ_L - C^\circ_M) = Dy - x\,[1 - A_{21}y^2 + E] - 2x^2EE \quad (I.3)$$

$$C^\circ_L = x\,[Ay + 2A_{21}y^2] + 2x^2Cy^2 + Dy \quad (I.4)$$

$$C^\circ_M = x\,[1 + Ay + A_{21}y^2 + E] + 2x^2[EE + Cy^2] \quad (I.5)$$

Recall that: x, y, A, A_{21}, C, D, E, EE are functions of the pH.

For a given pH, the numerical method consists to start from an initial x_0 value. x_0 can be chosen equal to the final solution x' of the above system (I.1-I.5) obtained for the previous pH' = pH – ΔpH. After n iterations, we define:

$$x(n) = x_0 \pm n\Delta x. \text{ Thus: } y(n) = {}^{1} = 0.5[-D(n) + \Delta(n)^{1/2}](x(n)A_{21})^- \quad (I.6)$$

The convergence is reached when both x(n), y(n) values verify Eqs.(I.4 and I.5); within a given precision: %Px = 100[x(n) – x(n-1)]/x(n). If it is not the case, we proceed in the same manner with the next x(n+1), y(n+1) values. It is obvious that the precision %Px of these solutions is increased when the step Δx is very small. However, this precision is limited by the precision of calculation of the computer. In general, our convergence precision is less than 1% which is comparable to the estimated error on the concentrations.

APPENDIX II ANALYTICAL RESOLUTION OF THE EQUATIONS OF CONSERVATION

The system of the conservation equations given in paragraph 4.3 could be reduced to an algebraic equation in "x" of degree 4, if we ignore the following species: $[(UO_2)_2(OH)]^{3+}$, $[(UO_2)_2(OH)_2]^{2+}$ $[(UO_2)(HCit)_2]^{4-}$ ($\beta_{12} = 0$) and $[(UO_2)H_2(HCit)_2]^{2-}$ ($\beta_{122} = 0$). Therefore, $EE = A_{21} = 0$. With such an assumption, the system of the conservation equations becomes:

$$C^\circ_L = Axy + 2x^2Cy^2 + Dy \quad (II.1)$$

$$C^\circ_M = x\,[1 + Ay + E] + 2x^2Cy^2 \quad (II.2)$$

$$\Delta C^\circ = (C^\circ_L - C^\circ_M) = Dy - x[1+E] \quad (II.3)$$

$$\text{Therefore, } y = (\Delta C^\circ + x[1+E])D^{-1} \quad (II.4)$$

$$\text{And: } x^4 + a_1x^3 + a_2x^2 + a_3x + a_4 = 0 \quad (II.5)$$

a_1	a_2	a_3	a_4
$2\Delta C_M(1+E)^{-1}$	$D^{-2}[2C(\Delta C_M)^2+A(1+E)D](a_0)^{-1}$	$[1+E+A(\Delta C_M)D^{-1}](a_0)^{-1}$	$(-C_M)(a_0)^{-1}$

With $a_0 = 2C(D^{-2})(1+E)^2$

The previous Eq. (II.5) can be factorized as following:

$$x^4 + a_1x^3 + a_2x^2 + a_3x + a_4$$
$$= (x^2 + x S_m + P)(x^2 + xS'_m + P') = 0 \quad \text{(II.6)}$$

After identification we obtain:

$$(S_m + S'_m) = a_1;\ (S_m.S'_m + P + P') = a_2;\ (P'.S_m + PS'_m) = a_3;$$
$$P.P' = a_4 \quad \text{(II.7)}$$

If now we define the parameter "z" as:

$$z = (P + P') \quad \text{(II.8)}$$

We can therefore express the parameters S_m, S'_m, P and P' in terms of "z" and the "a_1, a_2, a_4" coefficients:

$$S_m = 0.5[z - (z^2 - 4a_4)^{1/2}]\ ;\ S'_m = 0.5[z + (z^2 - 4a_4)^{1/2}] \quad \text{(II.9)}$$
$$P = 0.5[a_1 + \{(a_1)^2 - 4a_2 + 4z\}^{1/2}]\ ;$$
$$P' = 0.5[a_1 - \{(a_1)^2 - 4a_2 + 4z\}^{1/2}] \quad \text{(II.10)}$$

Now, the condition on the "a_3" coefficient $(P'.S_m + PS'_m) = a_3$ shows that "z" is solution of the following equation (of third degree) in z:

$$z^3 + A_1z^2 + A_2z + A_3 = 0 \quad \text{(II.11)}$$

With: $A_1 = -a_2$; $A_2 = (a_1a_3 - 4a_4)$;

$$A_3 = [4a_2a_4 - (a_3)^2 - (a_1)^2a_4] \quad \text{(II.12)}$$

The "z" real solutions depend on the sign of the determinant D_t:

$$D_t = Q^3 + R^2;\ Q = [3A_2 - (A_1)^2]/9\ ;$$
$$R = [9A_1A_2 - 27A_3 - 2(A_1)^3]/54 \quad \text{(II.13)}$$

$D_t > 0$	$D_t = 0$	$D_t < 0$
$z = S + T - A_1/3$	$z = (S + T)/2$	$z = 2(-Q)^{1/2}\mathrm{Cos}\{(\theta/3) + n\pi/3\} - A_1/3$; $(n = 0, 2, 4)$ $\mathrm{Cos}(\theta) = \pm R.(-Q^3)^{-1/2}$

with: $S = [R + (D)^{1/2}]^{1/3}$ and $T = [R - (D)^{1/2}]^{1/3}$ (II.14)

Finally, the four "x" solutions relatively to the Eq. (II.5) are:

$$x_{1+} = 0.5[-S_m + (\Delta)^{1/2}]\ ;\ x_{1-} = 0.5[-S_m - (\Delta)^{1/2}] \quad \text{(II.15)}$$
$$x'_{1+} = 0.5[-S'_m + (\Delta')^{1/2}]\ ;\ x'_{1-} = 0.5[-S'_m - (\Delta')^{1/2}] \quad \text{(II.16)}$$
with: $\Delta = [(S_m)^2 - 4P]^{1/2}$: $\Delta' = [(S'_m)^2 - 4P']^{1/2}$ (II.17)

Only *one* solution "x" is physically correct, because $x \equiv [UO_2^{2+}] \equiv [M]$ must be *positive* and must verify the condition of conservation of the total mass of both UO_2 and HCit. The corresponding "y" value is:

$$y \equiv [HCit^{3-}] \equiv [L] = (\Delta C_M + x[1+E])/D \quad \text{(II.18)}$$

REFERENCES

[1] Li. N. C. Lindenbaum, A. J. M. White: Some Metal Complexes of Citric and Tricarballylic Acids. J, Inorg. Nucl. Chem. 12, 122 (1959).

[2] Feldman, C. A. North, H. B. Hunter: Equilibrium Constants for the Formation of PolyNuclear Tridentate 1:1 Chelates in Uranyl-Malate, -Citrate and – Tartrate Systems. J. Am. Chem. Soc. 64, 1224 (1960).

[3] K. S. Rajan, A. E. Martell: Equilibrium Studies of Uranyl Complexes. Interaction of Uranyl Ion with Citric Acids, Inorg. Chem. 4, 462 (1965).

[4] G. Markovits, P. Klotz, L. Newman: Formation Constants for the Mixed-Metal Complexes between Indium (III) and Uranium (VI) with Malic, Citric, and Tartaric Acids, Inorg. Chem. 11 2405 (1972).

[5] Martell, R. M. Smith: Critical Stability Constants. Vol 3, Plenum Press, Texas (1989).

[6] Grenthe, J. Fuger, R. J. M. Konings, R. J. Lemire, A.B. Muller, C. Nguyen-Trung and H. Wanner: Chemical Thermodynamics of Uranium, Elsevier, North-Holland imprint (2003).

[7] Trémillon: Electrochimie analytique et Réactions en Solution, Masson, Paris (1993).

[8] J. J. Lenhart, S. E. Cabaniss, P. Mac Carthy, B. D. Honeyman: Uranium (VI) Complexation with Citric, humic and fulvic acids. Radiochim. Acta 88, 345 (2000).

[9] S. P. Pasilis, J. E. Pemberton: Speciation and Coordination Chemistry of Uranyl(VI)-Citrate Complexes in Aqueous Solutions, Inorg.Chem. 42, 6793 (2003).

[10] W. Hummel et al.: Chemical Thermodynamics of compounds and complexes of U, Np, Pu, Am, Tc, Se, Ni, and Zr with selected organic ligands, Elsevier, Amsterdam (2005).

[11] P. Gareil: L'électrophorèse de zone et la chromatographie électrocinétique capillaire, Analysis. 18, 221 (1990).

[12] B. Fourest, V. Sladkov: Transport methods as complementary tools for speciation purposes, Radiochim. Acta.93, 653 (2005).

[13] V. Sladkov, B. Fourest, S. M'Halla: Simultaneous determination of some activation and fission products in nitric acid solutions by capillary electrophoresis. ATALANTE, Nîmes, France (2004).

[14] E. H.Bailey, J. F. W. Mosselmans, P. F. Schofield: Uranyl-citrate speciation in acidic aqueous solutions an XAS study between 25 and 200 °C, Chemical Geology. 216, 1 (2005).

[15] J. M'halla, R. Besbes, R. Bouazzi, S. Boughammoura., S.: About the singular behaviour of the ionic condensation of sodium chondroitin sulphate, J. Chem. Phys. 321, 10 (2005).

[16] S. Boughammoura, J. M'Halla, B. Fourest: Application of capillary electrophoresis to the uranyl/citrate system in moderately acidic solutions, J. Radioanalytical and Nuclear Chemistry. 280, 547 (2009).

[17] J. P. Hunt: Metal Ions in aqueous solution, W. A. Benjamin, INC, N. Y (1963).